Angle-resolved photoelectron spectroscopy of atomic oxygen

P. van der Meulen* and M. O. Krause
Oak Ridge National Laboratory, Chemistry Division, P.O. Box 2008, Oak Ridge, Tennessee, 37831-6201

C. A. de Lange
Laboratory for Physical Chemistry, University of Amsterdam, Nieuwe Achtergracht 127, 1018 WS Amsterdam, The Netherlands
(Received 11 January 1991)

Using synchrotron-radiation-based angle-resolved photoelectron spectroscopy, the relative partial photoionization cross sections for the production of the $^4S^o$ and $^2D^o$ ionic states in atomic oxygen, as well as the corresponding asymmetry parameters, are measured from threshold at 13.62 to about 30 eV. The cross sections are placed on an absolute scale using previous data obtained with an electron spectroscopy modulation method. Attention is focused on the numerous autoionization resonances below the $2p^{-1}\,^2D^o$, $2p^{-1}\,^2P^o$, and $2s^{-1}\,^4P^e$ limits. The behavior of the asymmetry parameters across these resonances is observed for the first time. The $2s2p^4(^4P^e)3p\,(^3S^o,^3P^o,^3D^o)$ resonances are fitted by a Fano-type profile to obtain accurate values for the position, width, and q parameter.

I. INTRODUCTION

Photoelectron spectroscopy has long been used to study the electronic structure of both the parent atom (molecule) and its ion, and the interplay between theory and experiment greatly contributed to the understanding of many-electron effects. At first, attention was focused on the rare gases which are easily accessible experimentally and whose closed-shell nature made calculations tractable. However, in order to obtain good agreement between theory and experiment for the partial photoionization cross section (σ_i) and the asymmetry parameter (β_i), even for these relatively simple systems, it proved essential to include the detailed coupling between the various open and closed channels. Open-shell atoms (e.g., chalcogens, halogens), on the other hand, are believed to provide a much more stringent test for both theory and experiment. From the theoretical point of view the coupling between the multiplet states generated upon removal of a single electron is, especially at low photoelectron kinetic energy, of crucial importance. Experimentally, the reactive and transient nature of these species often causes complex problems in the determination of σ_i and β_i. Nevertheless, it is clear that our knowledge of electron correlation will greatly benefit from a detailed comparison between theoretical and experimental results for these systems. It is therefore not surprising that a lot of effort, albeit mostly theoretical, has been devoted to the study of the photoionization of atomic oxygen.[1–59]

The first calculation of the total photoionization cross section was reported in 1939 by Bates *et al.*,[1] and subsequently many authors have published improvements.[2–31] The correct treatment of exchange was included by Bates and Seaton,[5] while the coupling between open channels was first added by Henry.[9] Henry[12] also pioneered the inclusion of the effect of autoionization on σ_i and β_i. Several other papers dealing with autoionizing resonances have been published since then.[19,20,22,30,31]

Despite the large number of theoretical publications that have appeared in the literature, the amount of theoretical work done on partial cross sections or branching ratios[7,9,15,17,19,22,23,25,26] and asymmetry parameters[17–19,25,29] is still rather limited, especially when calculations extending beyond the independent-particle approximation[19,22,26,29] are considered.

The first He I α photoelectron spectrum of atomic oxygen was presented by Jonathan *et al.*[37,38] Subsequently the branching ratios for the production of the $^4S^o$, $^2D^o$, and $^2P^o$ ionic states as well as the asymmetry parameters were measured at the discrete Ne I, He I, and He II wavelengths.[41,47,48] So far, the only photoelectron spectroscopic study employing the continuum of synchrotron radiation is the one by Hussein *et al.*[52]

Several attempts[32,36,49,53–56] have been made to measure the absolute photoionization cross section of oxygen atoms, most recently by Angel and Samson,[54,56] who extended the work of Samson and Pareek.[53] In both cases a mass-resolved ion-detection technique was used. However, their results differ by a substantial amount from the value at 584 Å obtained by Van der Meer *et al.*,[55] who employed an electron spectroscopy modulation method.

It is well known that autoionization phenomena can strongly modify photoionization cross sections, and numerous groups have studied the formation and decay of autoionizing states below the $2p^{-1}\,^2D^o$ and $2p^{-1}\,^2P^o$ thresholds.[33–35,39,40,42,43,45,46,50,51] Only recently Angel and Samson[54,56] presented results for the Rydberg series converging upon the $2s^{-1}\,^4P^e$ limit. To date, no experimental data on the behavior of the asymmetry parameter across any of these resonances have been published.

At this point it is good to emphasize that, apart from its intrinsic physical interest, photoionization of atomic oxygen by solar radiation plays a vital role in the Earth's upper atmosphere. For a better understanding of a

variety of chemical and physical atmospheric processes the knowledge of the two basic photoionization parameters (σ_i,β_i) as a function of photon energy is of utmost importance. In this study we combined angle-resolved photoelectron spectroscopy and synchrotron radiation to study the partial photoionization cross sections, and the corresponding asymmetry parameters, for the production of the $^4S^o$ and $^2D^o$ ionic states between threshold at 13.62 and approximately 30 eV. Special attention was paid to the autoionization regions just below the $^2D^o$, $^2P^o$, and $^4P^o$ limits. A preliminary account of our work in the $^4P^e$ autoionization region has been presented earlier.[57]

II. EXPERIMENT

Our electron spectrometry with synchrotron radiation studies were carried out at the Aladdin storage ring in Wisconsin with a spectrometer described in detail before.[60,61] Only a concise account will be given here.

The apparatus contains three electrostatic analyzers mounted at right angles to each other on a rotatable platform which in itself is perpendicular to the incoming photon beam. In this arrangement and within the dipole approximation the following relation holds for the measured intensity $I_i(\theta)$ of the photoelectrons ejected from level i at an angle θ with respect to the main polarization direction:[62]

$$I_i(\theta)\sim\frac{d\sigma_i}{d\Omega}=\frac{\sigma_i}{4\pi}[1+\tfrac{1}{4}\beta_i(1+3p\cos 2\theta)]\ . \tag{1}$$

In this formula $d\sigma_i/d\Omega$ is the differential partial cross section, σ_i and β_i represent the angle-integrated partial cross section and the asymmetry parameter for level i, and p stands for the degree of linear polarization of the synchrotron radiation.

From Eq. (1) it is clear that the partial cross section σ_i can be obtained directly at the so-called magic angle θ_m:

$$\theta_m=\tfrac{1}{2}\arccos[(3p)^{-1}]\ . \tag{2}$$

The asymmetry parameter β_i can be calculated from

$$\beta_i=4(R_i-1)/[3p(R_i+1)-(R_i-1)]\ , \tag{3}$$

where R_i is the ratio of the intensities measured parallel and perpendicular to the polarization vector. Because of the positioning of the analyzers these intensities can be measured simultaneously. Using the asymmetry parameter derived in this manner the cross section can then be extracted from the measurements taken at either 0° or 90° with the aid of Eq. 1. In general, the agreement between this scheme and the direct measurement of σ_i (Eq. 2) was excellent.

In order to produce oxygen atoms, molecular oxygen of purity greater than 99.999% was subjected to a 2.45-GHz microwave discharge using a Microtron 200, Mark 3 power generator (Electron Medical Supplies Ltd.). The discharge was triggered by a high-voltage spark, and was maintained in an 11-mm-diam phosphorous pentoxide coated quartz tube. To prevent rapid deterioration of the coating the microwave cavity was air cooled. However, the cooling was kept to a minimum to increase the oxygen atom yield. The dissipated microwave power amounted to about 100 W. Under these conditions the amount of excited molecular oxygen $O_2(^1\Delta_g)$ produced[37] proved to be small. The resulting gas mixture flowed into the ionization chamber through a 11-mm-diam Pyrex tube coated with halocarbon wax to suppress wall recombination reactions. The distance between the discharge and the ionization region was approximately 30 cm. No evidence for excited *atomic* species[34] was found. A schematic view of the experimental setup is given in Fig. 1.

Because only about 20% of the O_2 molecules entering the discharge are dissociated, two sets of experiments were performed, viz. one set with the microwave discharge on and another with the discharge off. From those two measurements it is then possible to obtain spectra of atomic oxygen virtually free of $O_2(^3\Sigma_g^-)$ signals by a suitable subtraction procedure.[63]

Measurements were normally performed in the constant ionic state (CIS) mode[64] in which both the photon energy and the photoelectron energy are scanned synchronously as to stay on top of a chosen peak in the photoelectron spectrum. Conventional photoelectron (PE) spectra were used to correct for the decay of the photon flux with time and for pressure variations in the source cell, as well as to relate different CIS scans to each other. Both CIS and PE spectra were taken in the constant pass energy mode, i.e., by scanning the (de)accelerating voltage which the photoelectrons pass before entering the analyzers. The pass energy was typically 12.5 eV. The resolution of the electron analyzers was nominally set to $\Delta E/E=0.01$. In this way only *relative* partial cross sections are measured. They can be put on an absolute scale using data available in the literature.[32,36,49,53–56]

The experiments described in this work were performed during two experimental periods on two different beamlines, namely a 4-m normal-incidence monochromator (NIM) equipped with a 1200-l/mm gold-coated grating and a 1-m Seya-Namioka monochromator in which a 1440-l/mm osmium-coated grating was installed. In both cases the bandpass of the monochromator, which in a CIS scan is the only factor contributing to the overall resolution, was normally set to about 0.7 Å. The monochromators were calibrated against the well-known Xe

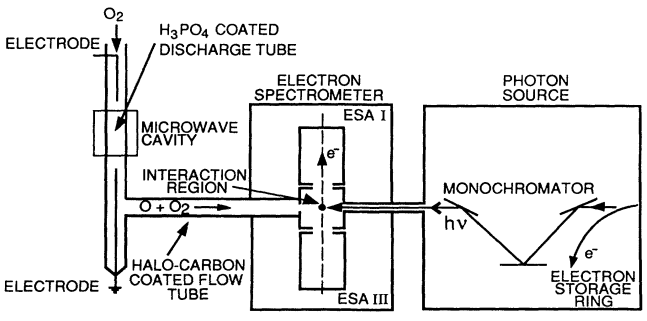

FIG. 1. Schematic view of the experimental apparatus.

$5p^6 \rightarrow 5p^5(^2P_{1/2})ns'/nd'$ and Ar $3s^23p^6 \rightarrow 3s3p^6(^2S_{1/2})np$ resonance lines,[65,66] and the atomic oxygen lines for which the energy is accurately known.[33,45,51] To determine the setting for the magic angle θ_m [Eq. (2)] it is necessary to obtain both the degree of polarization and the orientation of the main polarization vector, which may be tilted out of the horizontal plane of the storage ring due to the interaction with various optical components. This was done by measuring PE spectra as a function of the angle θ for a photoline with a high β value, e.g., Xe $5p$ at 21.22 eV.[67] The tilt angle amounted to 15° on the 4-m NIM, and 0° for the 1-m Seya-Namioka beamline.

Rare-gas calibration measurements served to determine the polarization of the photon beam and a correction factor which includes the inhomogeneity of the source volume and the differences between the response functions of the analyzers. Using several rare-gas lines at photon energies at which the asymmetry parameter is known to an accuracy of better than 0.05, e.g., Ar $3p$, Kr $4p$ and Xe $5p$ at 21.22 eV (Ref. 67) and Ar $3p$ at 16.53 eV,[68] we found a polarization of $p = 0.77 \pm 0.03$ for the NIM and 0.90 ± 0.01 for the Seya-Namioka beamline. The above correction factor, which is used for the accurate determination of the asymmetry parameter, is believed to be constant at high photoelectron kinetic energies, but may vary when the ionization thresholds are approached. To study its low-energy behavior CIS scans between the Xe $5p^{-1}\,^2P_{1/2}$ and $^2P_{3/2}$ limits were recorded.[65] No erroneous results were found for electron kinetic energies greater than about 0.5 eV. All calibrations were repeated several times during the experimental periods.

The relative partial cross section can then be obtained from

$$\sigma_i \sim I_i(\theta_m)/N(h\nu) , \tag{4}$$

where $N(h\nu)$ is the (relative) number of photons at a particular photon energy. The function $N(h\nu)$ was determined by the photoelectron for analysis of x rays method[69] in which the well-known cross sections of the Xe $5p$ and Ar $3p$ levels were used.[70,71]

III. RESULTS AND DISCUSSION

The ground-state configuration of atomic oxygen corresponds to $2s^22p^4(^3P^e)$. Removal of a $2p$ electron leads to the $2s^22p^3(^4S^o)$, $2s^22p^3(^2D^o)$, and $2s^22p^3(^2P^o)$ ionic states at 13.62, 16.94, and 18.64 eV, respectively.[33,45] On the other hand, the ejection of a $2s$ electron gives rise to the $2s2p^4(^4P^e)$, $2s2p^4(^2D^e)$, $2s2p^4(^2S^e)$, and $2s2p^4(^2P^e)$ ionic states at 28.49, 34.20, 37.88, and 39.98 eV.[51]

Usually there are several optically allowed Rydberg series associated with each ionization limit. Apart from the ones converging upon the lowest ionic state, the individual Rydberg levels can, selection rules permitting, autoionize into the available continua. Hence we can anticipate extensive autoionizing structure, both in the partial cross sections (Beutler-Fano profiles) and in the asymmetry parameters, in the extreme ultraviolet spectra of oxygen atoms. However, because the photon flux of the monochromators used in this work dropped rapidly above 30 eV, only the resonances below the $^2D^o$, $^2P^o$, and $^4P^e$ limits could be studied.

TABLE I. Optically permitted Rydberg series and the continua into which they are allowed to autoionize assuming *LS* coupling is valid.

Series	Continua
$2s^22p^3(^2D^o)ns\ ^3D^o$	$^4S^o\varepsilon d$
$nd\ ^3S^o$	$^4S^o\varepsilon s$
$^3P^o$	none
$^3D^o$	$^4S^o\varepsilon d$
$2s^22p^3(^2P^o)ns\ ^3P^o$	$^2D^o\varepsilon d$
$nd\ ^3P^o$	$^2D^o\varepsilon d$
$^3D^o$	$^4S^o\varepsilon d$, $^2D^o\varepsilon s/\varepsilon d$
$2s2p^4(^4P^e)np\ ^3S^o$	$^4S^o\varepsilon s$, $^2D^o\varepsilon d$
$^3P^o$	$^2D^o\varepsilon d$, $^2P^o\varepsilon s/\varepsilon d$
$^3D^o$	$^4S^o\varepsilon d$, $^2D^o\varepsilon s/\varepsilon d$, $^2P^o\varepsilon d$

An energy diagram of the relevant levels in this region is given in Fig. 2. Table I lists the optically permitted Rydberg series and, within the *LS* coupling scheme, the continua in which they are allowed to autoionize. Unfortunately, due to the limited resolution in the PE spectra, which did not allow us to separate the weak $^2P^o$ photoline

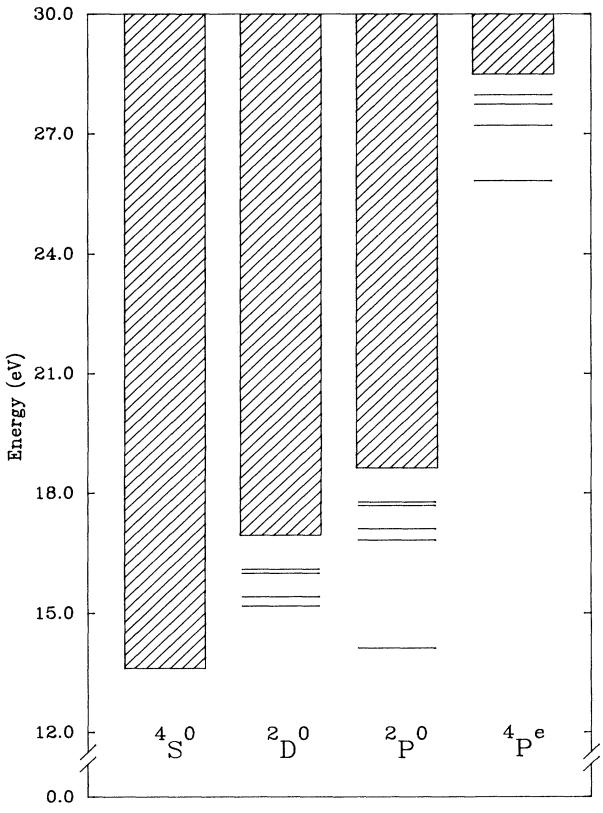

FIG. 2. Energy-level diagram of atomic oxygen. Only the four lowest ionic states together with members of several autoionizing Rydberg series are shown.

from the interfering O_2 spectrum, no reliable measurements for the $^2P^o$ ionic state could be obtained. Thus, from the three energetically accessible states, only results for the $^4S^o$ and $^2D^o$ levels are presented.

As mentioned before, only *relative* partial cross sections were measured. Our relative values, however, were put on an *absolute* scale using the results of Van der Meer *et al.*[55] at 584 Å [$O^+(^4S^o)$, 2.4 Mb; $O^+(^2D^o)$ 3.6 Mb], which we believe are more accurate than those given by Samson and Pareek.[53]

In the present experiment at the Synchrotron Radiation Center we obtained essentially the same results as those reported by Van der Meer *et al.*, although our error bars were somewhat larger. In addition, the ratio between the partial cross sections for the $O_2(^3\Sigma_g^-) \rightarrow O_2^+(^2\Pi_g)+e^-$ and the $O_2(^1\Delta_g) \rightarrow O_2^+(^2\Pi_g)+e^-$ transitions as reported by Van der Meer *et al.*, was recently corroborated by experiments at 584 Å performed by Cockett.[59]

In order to remove interfering signals arising from ground-state molecular oxygen $O_2(^3\Sigma_g^-)$ a subtraction procedure was applied. Its effectiveness is illustrated in Fig. 3. At the photon energy at which these spectra were taken (17.1 eV) autoionization in the oxygen molecule[72–85] leads to the population of high vibrational levels in the $O_2^+(^2\Pi_g)$ ionic state which overlap with the $O^+(^4S^o)$ band. However, from Fig. 3 it is clear that in the combination spectrum the contribution of the $O_2(^3\Sigma_g^-) \rightarrow O_2^+(^2\Pi_g)+e^-$ transition is almost completely removed.

Over the whole region surveyed in this study, the uncertainty in our relative partial cross sections is approximately 20% as evaluated from such factors as the reproducibility of the spectra and the uncertainty in the determination of the photon flux as a function of energy. The possible error in the absolute partial cross section depends, of course, on the accuracy of the normalization standard. Van der Meer *et al.*[55] only quoted the statistical scatter in their experimental cross-section ratios, which amounted to ±3%. Therefore, barring systematic errors in the normalization standard, our absolute cross sections are correct to approximately 20%.

The error limits (one standard deviation) for the asymmetry parameters can, in general, be put at ±0.10. This estimate includes the statistical error as well as the uncertainty in the relative efficiencies of the analyzers and the polarization.

This section is divided into four parts, three dealing with the autoionizing resonances below the $^2D^o$, $^2P^o$, and $^4P^e$ limits, and another in which the structureless region between approximately 19.0 and 25.0 eV is addressed.

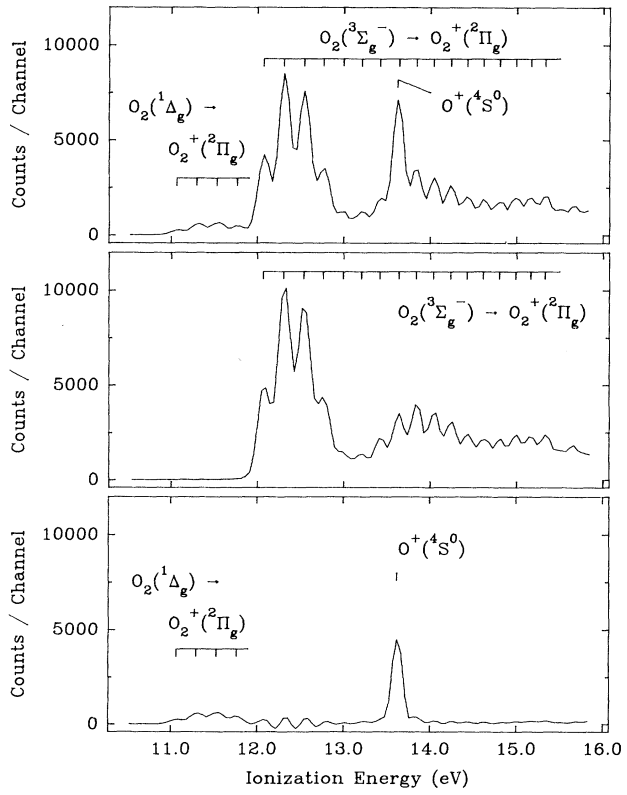

FIG. 3. Photoelectron spectra at a photon energy of 17.10 eV and at an angle of 0° with respect to the main polarization vector. Upper panel, discharge on; center panel, discharge off; lower panel, linear combination of discharge-on and discharge-off spectra in which the signal due to the $O_2(^3\Sigma_g^-) \rightarrow O_2^+(^2\Pi_g)+e^-$ transition has been removed. The spectra contain about 120 points each.

A. Resonances below the $^2D^o$ threshold

The absolute photoionization cross section for the $^4S^o$ channel between the first ionization energy at 13.62 and about 17 eV is presented in Fig. 4. Since the $^4S^o$ ionic ground state is the only state accessible, this value represents the total photoionization cross section, and

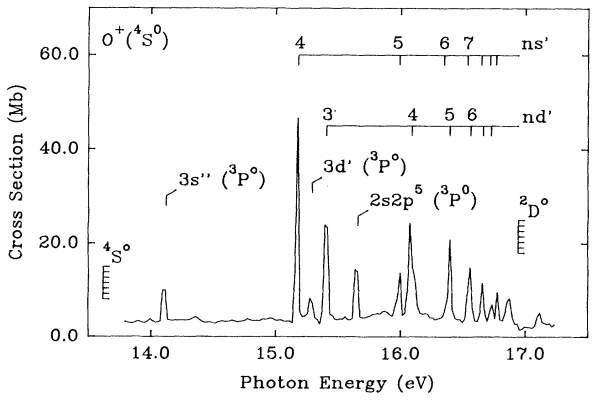

FIG. 4. Absolute photoionization cross section for the $^4S^o$ ionic state between the $^4S^o$ threshold at 13.62 eV and the $^2D^o$ threshold at 16.94 eV. The CIS spectrum has been taken in steps of 20 meV and with a resolution of 0.7 Å. The spectrum is normalized to the absolute cross section at 21.22 eV as described in the text.

can be directly compared with ion measurements in the same region.[40,43,46,53,54,56] The data in Fig. 4 were taken at a resolution of approximately 0.7 Å. In order to accommodate the complete region between the $^4S^o$ and $^2D^o$ limits in one scan, a rather coarse step size of 20 meV/point was chosen. Resonances due to the $ns'(^2S^o,^3P^0,^3D^o)$, and $ns''(^3P^o)$ series as well as the $2s^22p^4(^3P^e)\rightarrow 2s2p^5(^3P^o)$ inner valence shell excitation are clearly seen.

The same part of the spectrum was studied at much higher resolution by Dehmer *et al.*,[40,43,46] who employed a mass-resolved ion-detection technique. These authors concentrated on the resonances of $^3P^o$ symmetry, which, assuming Russell-Saunders (*LS*) coupling is valid, are forbidden to autoionize, and did not report absolute values. By contrast, Samson and Pareek[53] and Angel and Samson[54,56] presented absolute photoionization cross sections, but omitted the resonance features from their data.

Based on the results of Van der Meer *et al.*[55] our values for the absolute photoionization cross section close to the $^4S^o$ threshold are about 15% lower than those predicted by a sophisticated calculation recently done by Bell *et al.*[31] In good agreement with this calculation, we find that the nonresonant cross section stays virtually constant when the ionization threshold is approached. This is in contrast to the results of Samson and Pareek[53] and Angel and Samson,[54,56] who measured a significant drop. The discrepancy between the relative experimental results in this region is as yet unresolved. It should be noted that theory is divided on this issue. The random-phase-approximation with exchange calculations of Vesnicheva *et al.*[29] and Orlov, Cherepkov, and Chernysheva[30] show the gradual decrease in the nonresonant cross section as observed by Samson and Pareek[53] and Angel and Samson,[54,46] while the *R*-matrix calculations of Taylor and Burke,[20] and Pradhan,[22] and Bell *et al.*[31] predict a similar trend as observed in the present work.

Figure 5 shows the absolute photoionization cross section and the asymmetry parameter for the $^4S^o$ ionic state in the region of the $3d'(^3S^o,^3D^o)$, $4s'(^3D^o)$, $3d'(^3P^o)$, and $2s2p^5(^3P^o)$ resonances. These data were taken at a resolution of 0.7 Å and a stepsize of 5 meV/point. In this range the determination of σ_i and β_i is often complicated by the overlap of the $O^+(^4S^o)$ and $O_2{}^+(^2\Pi_g)$ bands in the PE spectra. Although these bands are normally well separated, autoionization in the molecule leads to the

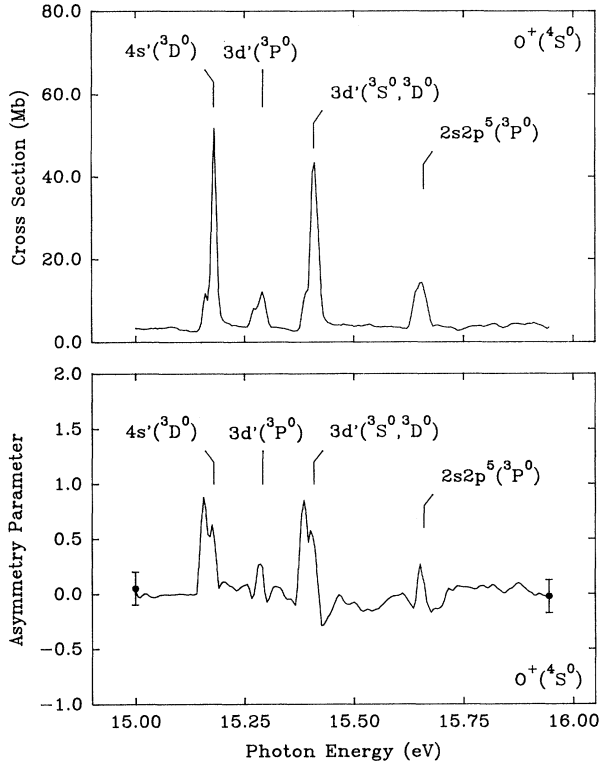

FIG. 5. Absolute photoionization cross section (upper panel) and asymmetry parameter (lower panel) for the $^4S^o$ ionic state across the $4s'$ and $3d'$ resonance region. The CIS spectra have been taken in steps of 5 meV. The resolution of 0.7 Å was insufficient to fully separate the different (J',J'') pairs associated with each transition. The indicated positions are an average over all J levels.

population of very high vibrational levels in the ion,[72–85] thereby partly obscuring the $O^+(^4S^o)$ band. In this case, the autoionization proceeds most likely through Rydberg levels converging upon the $O_2{}^+(^4\Pi_u)$ state at 16.101 eV.[76,78,85] Generally, the subtraction procedure outlined above almost completely removed the $O_2{}^+$ contribution (where applicable), but sometimes, at a particularly strong resonance, some traces remained. Thus both the asymmetry parameter and the partial cross section show

TABLE II. Resonance parameters for the $4s'(^3D^o)$ and $3d'(^3S^o,^3D^o)$ autoionizing states. *L* stands for a calculation in the length formulation, *V* represents a calculation in the velocity gauge.

	Energy (eV)				FWHM (meV)			*q* parameter		
Resonance state	Ref. 12 Theor.	Ref. 19 Theor.	Ref. 20 Theor.	Ref. 45 Expt.	Ref. 12 Theor.	Ref. 19 Theor.	Ref. 20 Theor.	Ref. 12 Theor.	Ref. 19 Theor.	Ref. 20 Theor.
$4s'(^3D^o)$	15.229	15.229	15.274	15.179	0.093	0.094	0.088	61.2	−57.6 (*L*) −41.7 (*V*)	~40
$3d'(^3S^o)$	15.428		15.418	15.416	0.102		0.109	61.8		62.5 (*L*) 69.6 (*V*)
$3d'(^3D^o)$	15.423		15.410	15.406	0.389		0.436	20.2		16.6 (*L*) 17.7 (*V*)

a somewhat larger scatter than noted in the other spectra.

When compared with the results of Dehmer *et al.*[43,46,48] it is clear that we find a much lower intensity for resonances of $^3P^o$ symmetry. Even though this may be partly caused by differences in resolution and the mesh with which the resonances were scanned, the main reason for the high intensity of the $^3P^o$ resonances in the spectra of Dehmer *et al.* could lie in the presence of traces of oxygen in their helium discharge lamp. Because the $^3P^o$ states are forbidden to autoionize within an *LS* coupling scheme (see Table I), they decay partly by emission, and the addition of only a small amount of oxygen to the lamp gas leads to the selective population of the $^3P^o$ states.[42,50] States of $^3S^o$ or $^3D^o$ symmetry decay solely by autoionization and are therefore not enhanced.

The resonances in Fig. 5 have been the subject of several theoretical treatments, the results of which are summarized in Table II. None of these studies incorporated spin-orbit coupling, hence the $^3P^o$ resonances were not included and the fine structure of the transitions, with the different (J',J'') pairs as much as 2 Å apart, was omitted. The calculations[12,19,20] predict a large value for the Fano line profile index[86–91] $|q|$, i.e., a Lorentzian line shape, which is supported by our experiment. Unfortunately, our resolution did not allow a detailed study of the fine-structure components of each transition.

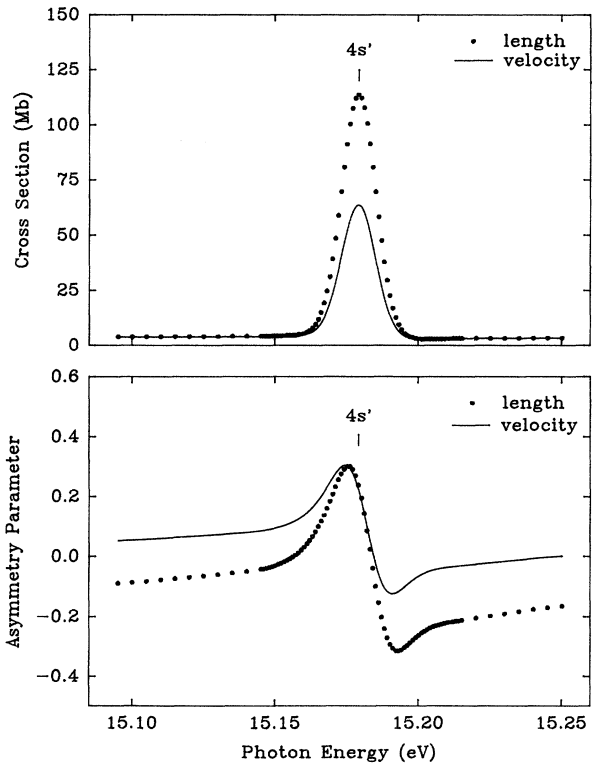

FIG. 6. Photoionization cross section (upper panel) and asymmetry parameter (lower panel) across the 4*s'* resonance as calculated by Smith (Ref. 19). In order to facilitate a comparison with our experimental values (see Fig. 5), the theoretical data have been convoluted by a Gaussian of 0.71-Å FWHM representing the monochromator slit function.

Figure 6 shows the result of a calculation by Smith[19] of the photoionization cross section and the asymmetry parameter across the $4s'(^3D^o)$ resonance. In order to facilitate a comparison with our experiment Smith's data have been convoluted by a Gaussian of 0.71-Å full width at half maximum (FWHM) representing the monochromator slit function. To the best of our knowledge this is the only calculation of the behavior of the asymmetry parameter across an autoionizing resonance in atomic oxygen. As can be seen from Figs. 5 and 6 the agreement for the cross section is quite good, especially in the velocity gauge. For the asymmetry parameter the agreement is less satisfactory, but again, the velocity form seems to be closer to the experimental values. The sign of the q parameter, which was found to be negative by Smith,[19] but is positive in all other calculations,[12,20] could not be established unambiguously from the experimental data.

The only other experimental value for the asymmetry parameter of the $O^+(^4S^o)$ ionic state below the $^2D^o$ threshold has been published by Samson and Hancock.[47] At the Ne I line (735.9 Å, 16.85 eV) they reported a value of 0.00 ± 0.02, which seems very reasonable when compared to our measurements, even though the Ne I line is close to the $12d'(^3S^o,^3P^o,^3D^o)$ resonance[35,45,51] so some autoionization may occur.

B. Resonances below the $^2P^o$ threshold

In this energy region both the $^4S^o$ and $^2D^o$ channels are open. The absolute photoionization cross sections and the asymmetry parameters for both ionic states are shown in Figs. 7 and 8. In the cross section of the $^2D^o$ state we observe strong $nd''(^3P^o,^3D^o)$ resonances, and a weaker $ns''(^3P^o)$ series, while in the $^4S^o$ channel we can only detect evidence for the $nd''(^3D^o)$ autoionizing lines as could have been expected on the basis of *LS* coupling. Surprisingly, the asymmetry parameter for the $^4S^o$ state shows virtually no sign of autoionizing resonances, though both the ns'' and nd'' series are easily identified in the $^2D^o$ channel.

A number of theoretical studies[12,20,22,31] concerning the resonances have been performed, although only the total cross section has been addressed. The results of some of these calculations are presented in Table III. We find a Lorentzian line shape for the nd'' series in both the $^4S^o$ and $^2D^o$ channels in agreement with the high $|q|$ value predicted by theory for the total cross section. The ns'' resonances, which are only visible in the $^2D^o$ channel, appear to have a negative q of about -2, again in good agreement with theory. Our resolution did not allow a detailed study of the width of these resonances, but especially the ns'' series appears to be broader than predicted by the calculations in Table III. Since none of the calculations for the asymmetry parameter in this range[17–19,25,29] incorporates the resonance structure, a comparison between theory and experiment with regard

TABLE III. Resonance parameters for the lower members of the Rydberg series converging upon the $^2P^o$ limit. L stands for a calculation in the length formulation, V represents a calculation in the velocity gauge. These values pertain to the total cross section.

Resonance state	Energy (eV) Ref. 12 Theor.	Energy (eV) Ref. 20 Theor.	Energy (eV) Ref. 45 Expt.	FWHM (meV) Ref. 12 Theor.	FWHM (meV) Ref. 20 Theor.	q parameter Ref. 12 Theor.	q parameter Ref. 20 Theor.
$5s''(^3D^o)$	17.703	17.722	17.687	3.39	0.648	−5.99	−2.113 (L)
							−2.971 (V)
$6s''(^3P^o)$	18.050	18.057	18.042	1.68	0.304	−5.56	−2.191 (L)
							−2.934 (V)
$3d''(^3P^o)$		17.115	17.103		≤0.01		
$4d''(^3P^o)$	17.780	17.777	17.775	1.48	≤0.01	−7.92	
$5d''(^3P^o)$	18.088	18.083	18.086	0.765	≤0.01	−7.47	
$3d''(^3D^o)$		17.110	17.105		0.265		−16.00 (L)
							−16.92 (V)
$4d''(^3D^o)$	17.780	17.775	17.775	1.25	0.123		−18.49 (L)
							−19.71 (V)
$5d''(^3D^o)$	18.088	18.083	18.086	0.686	0.066		−18.19 (L)
							−18.37 (V)

to β_i could not be made.

The good agreement between our intensity ratios, i.e., $\sigma(^2D^o)/\sigma(^4S^o)$, and those published by Hussein *et al.*[52] is illustrated in Table IV. Between the $^2D^o$ and $^2P^o$ thresholds our total nonresonant cross section, obtained by adding the partial cross sections of the $^4S^o$ and $^2D^o$ ionic states, is about 20% lower than the values calculated by Bell *et al.*,[31] as compared to a 15% smaller value below

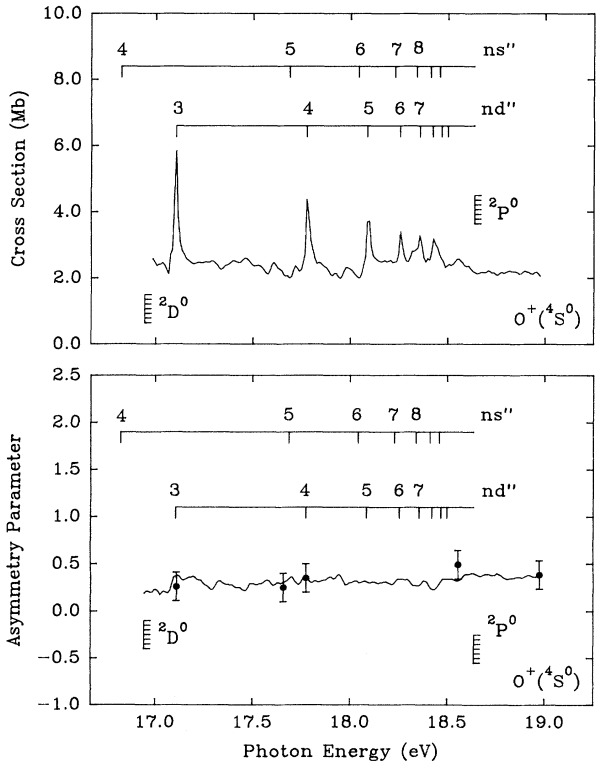

FIG. 7. Absolute photoionization cross section (upper panel) and asymmetry parameter (lower panel) for the $^4S^o$ ionic state between the $^2D^o$ threshold at 16.94 eV and the $^2P^o$ threshold at 18.64 eV. The CIS spectra have been taken in steps of 10 meV and with a resolution of 0.7 Å. The ns'' Rydberg series is indicated, but not observed in this channel.

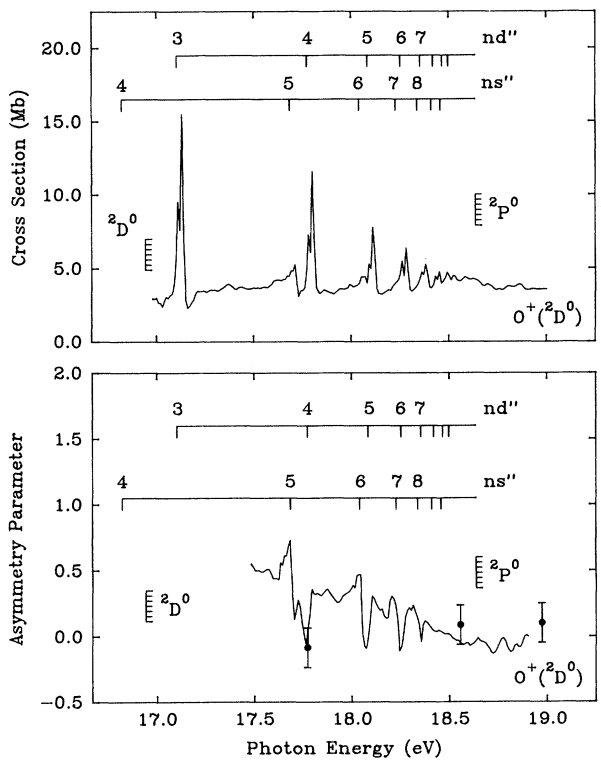

FIG. 8. Absolute photoionization cross section (upper panel) and asymmetry parameter (lower panel) for the $^2D^o$ ionic state between the $^2D^o$ threshold at 16.94 eV and the $^2P^o$ threshold at 18.64 eV. The CIS spectra have been taken in steps of 10 meV and with a resolution of 0.7 Å. The ns'' Rydberg series is clearly visible in this channel.

TABLE IV. Intensity ratio $[\sigma(^2D^o)/\sigma(^4S^o)]$ at selected photon energies outside the autoionization resonances.

Photon energy (eV)	$\sigma(^2D^o)/\sigma(^4S^o)$[a]	$\sigma(^2D^o)/\sigma(^4S^o)$[b]
17.22	1.12	1.13
17.59	1.57	1.43
17.92	1.43	1.53
18.28	1.87	1.72
18.79	1.65	1.70
19.08	1.63	1.57
19.37	1.63	0.97
19.68	1.61	1.61
20.00	1.56	1.64
20.66	1.51	1.77
21.38	1.51	1.50

[a]This work; estimated errors 10%.
[b]Reference 52. These data show an anomaly at 19.37 eV; errors quoted 15%.

the $^2D^o$ ionization limit. This indicates that Bell *et al.* correctly incorporated the $^2D^o$ channel, that opens at 16.94 eV.

Our experiment shows that the nonresonant cross section for both the $^4S^o$ and the $^2D^o$ components remains fairly constant between the $^2D^0$ and $^2P^o$ thresholds. Although this is supported by the R-matrix calculations of Pradhan[22] and Bell *et al.*,[31] it is in disagreement with the measurements of Angel and Samson,[54,56] who found a rise towards the $^2P^o$ limit. Again, the reason for the discrepancies between the different experimental relative cross sections is unclear. Finally, no experimental determination of the asymmetry parameters exists in this region to compare with the present results.

C. The structureless region between 19.0 and 25.0 eV

Since this region does not contain any autoionization resonances we expect a rather smooth curve for both the photoionization cross section and the asymmetry parameter. Our results for the $^4S^o$ and $^2D^o$ components are shown in Figs. 9 and 10, along with the available measurements at the He Iα wavelength.[32,36,47,53] Also shown are the results of several theoretical calculations which, at least to some extent, include the effect of electron correlation.[9,19,26,29] Our numerical values are presented in Table V.

Within the error limits, our results for the asymmetry parameter agree with the values given by Samson and Hancock,[47] even though theirs are slightly higher. No other experimental points exist in this region.

For the asymmetry parameter of the $^4S^o$ ionic state the agreement with theory is quite good. Although there is some discrepancy in the case of the $^2D^o$ component, the shape of the curve is very well represented by the calculation of Vesnicheva *et al.*[29] In both instances the theoretical values are too high compared with the present experimental ones.

It should be noted that most of the asymmetry parameter calculations at the Hartree-Slater or Hartree-Fock level[17,18,25] give results similar to the more sophisticated calculations shown in Figs. 9 and 10, indicating that, at least at these photon energies, electron correlation may not be all that important.

TABLE V. Experimental absolute photoionization cross sections (σ) and asymemtry parameters (β) for the $^4S^o$ and $^2D^o$ ionic states between 19.0 and 25.0 eV.

Photon energy (eV)	$\sigma(^4S^o)$ (Mb)	$\sigma(^2D^o)$ (Mb)	$\beta(^4S^o)$	$\beta(^2D^o)$
25.00	1.87	2.53	0.87	0.57
24.50	1.91	2.67	0.86	0.51
24.00	2.02	2.86	0.83	0.43
23.50	2.10	3.05	0.80	0.41
23.00	2.15	3.21	0.74	0.37
22.50	2.22	3.31	0.71	0.31
22.00	2.32	3.44	0.67	0.22
21.50	2.36	3.56	0.65	0.17
21.00	2.39	3.60	0.58	0.11
20.50	2.39	3.61	0.56	0.08
20.00	2.32	3.62	0.51	0.04
19.50	2.24	3.65	0.45	0.03
19.00			0.36	0.00

TABLE VI. Resonance parameters for the $2s \rightarrow 3p(^3S^o, ^3P^o, ^3D^o)$ autoionizing Rydberg states derived from the experimental profile. Details of the fit procedure are described in the text. The numbers in parentheses are estimated probable errors which include the uncertainty in the description of the monochromator slit function, and for the resonance energy, the energy calibration of the monochromator.

Ionic state	Resonance state	Energy (eV)	FWHM (meV)	q
$^4S^o$	$2s2p^4(^4P^e)3p(^3D^o)$	25.75(0.03)	8(1)	−2.1(0.1)
	$2s2p^4(^4P^e)3p(^3S^o)$	25.82(0.03)	2(1)	2.7(0.1)
$^2D^o$	$2s2p^4(^4P^e)3p(^3D^o)$	25.75(0.03)	13(1)	10(2)
	$2s2p^4(^4P^e)3p(^3S^o)$	25.83(0.03)	15(1)	4(1)
	$2s2p^4(^4P^e)3p(^3P^o)$	25.95(0.03)	32(1)	−0.7(0.1)

When plotted as a function of photoelectron kinetic energy (not shown), the asymmetry parameters for the $^4S^o$ and $^2D^o$ levels almost coincide, as predicted by the calculations of Manson *et al.*,[25] who showed that anisotropic effects, which would cause a difference between the two components, are small for second row atoms.

For the partial cross sections we find large discrepancies, not only between the experimental values,[33,36,47,53]

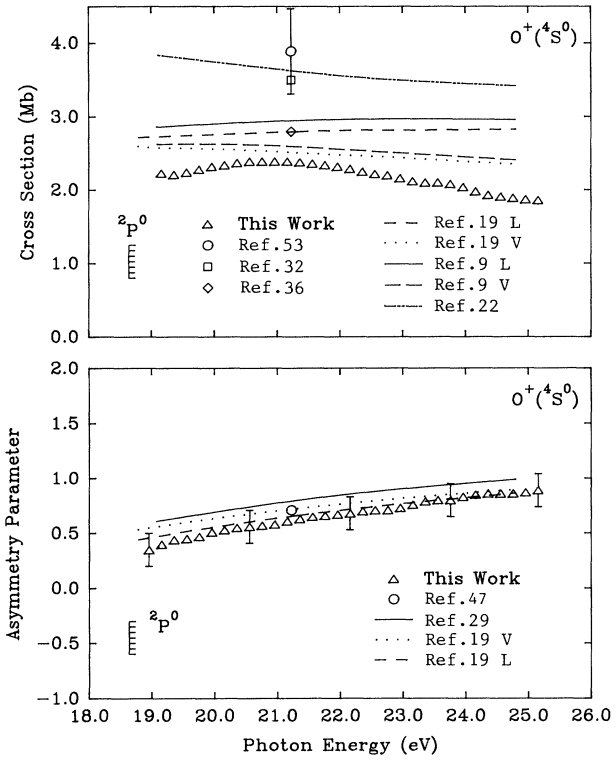

FIG. 9. Absolute photoionization cross section (upper panel) and asymmetry parameter (lower panel) for the $^4S^o$ ionic state between 19.0 and 25.0 eV. L and V stand for length and velocity results. The total cross sections at the He I α wavelength of Samson and Pareek (Ref. 53), Cairns and Samson (Ref. 32), and Comes, Speier, and Elzer (Ref. 36) have been broken down into partial cross sections using the branching ratios of Samson and Petrosky (Ref. 42). The uncertainties in these partial cross sections are 15%, 36%, and 16%, respectively. The experimental value for the asymmetry parameter of Samson and Hancock (Ref. 47) has an uncertainty of 0.02. Theoretical values are from Smith (Ref. 19), Henry (Ref. 9), Pradhan (Ref. 22), and Vesnicheva *et al.* (Ref. 29).

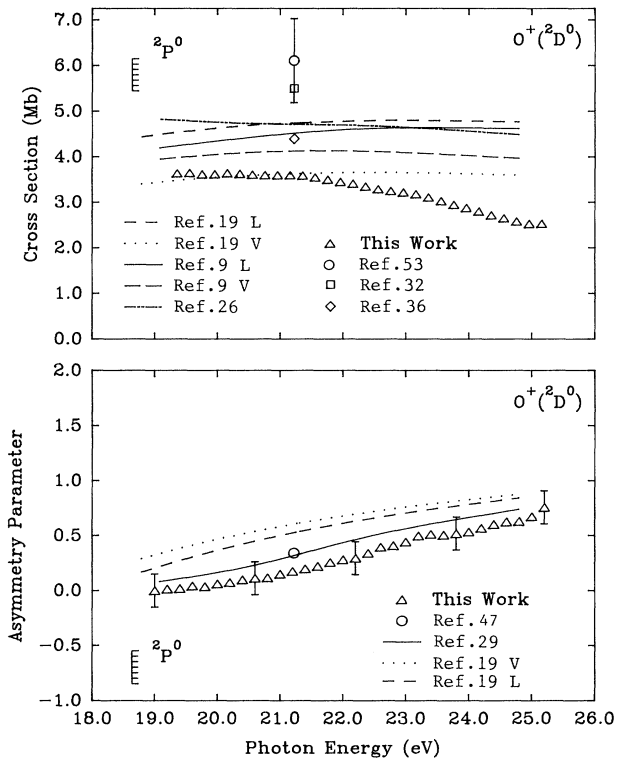

FIG. 10. Absolute photoionization cross section (upper panel) and asymmetry parameter (lower panel) for the $^2D^o$ ionic state between 19.0 and 25.0 eV. L and V stand for calculations in the length and velocity formulation. The total cross section at the He I α wavelength of Samson and Pareek (Ref. 53), Cairns and Samson (Ref. 32), and Comes, Speier, and Elzer (Ref. 36) have been broken down into partial cross sections using the branching ratios of Samson and Petrosky (Ref. 42). The uncertainties in these partial cross sections are 15%, 36%, and 16%, respectively. The experimental value for the asymmetry parameter of Samson and Hancock (Ref. 47) has an uncertainty of 0.05. Theoretical values are from Smith (Ref. 19), Henry (Ref. 9), Pradhan (Ref. 26), and Vesnicheva *et al.* (Ref. 29).

but also among the various calculations.[9,19,26,29] The disagreement between the calculations is not well understood since in this energy region even the relatively straightforward Hartree-Fock method should produce fairly accurate results.

Our results seem too low when compared with either the other experimental values, or the calculations. However, this may be caused by our choice of the measurements of Van der Meer *et al.*[55] as a normalization standard. From our experimental results it appears that the $^4S^o$ and $^2D^o$ partial cross sections are dropping toward higher energies, which, apart from the normalization factor, is confirmed by the most recent calculations on the partial cross sections by Pradhan.[22,26]

D. Resonances below the $^4P^e$ threshold

We reported on the resonances belonging to the $2s \rightarrow np (n \geq 3)$ Rydberg series in an earlier, preliminary paper.[57] Here we have put the cross sections for the $^4S^o$ and $^2D^o$ components on an absolute scale, and we have fitted the first ($n=3$) resonance with a Fano-type profile.

Figure 11 shows the absolute photoionization cross section for the $^4S^o$ and $^2D^o$ ionic states across the np Rydberg series. As pointed out before[57] (Table I), the first member of the series shows evidence for only the $2s2p^4(^4P^e)3p(^3S^o)$ and $2s^22p^4(^4P^e)3p(^3D^o)$ lines in the $^4S^o$ channel, whereas in the $^2D^o$ channel all three $2s^22p^4(^4P^e)3p(^3S^o,^3P^o,^3D^o)$ autoionizing states are observed. For the higher members of the series ($n>3$) the individual states are no longer resolved. It should be noted that, just as for the resonances below the $^2P^o$ threshold, here LS coupling also seems to be appropriate. This is in contrast to the resonance below the $^2D^o$ limit, where a breakdown of the LS coupling scheme occurs.

In order to obtain more accurate values for the position, the width and the Fano line profile index q for the individual resonances we have fitted the $n=3$ member of the series with a Shore profile,[92–94] while taking into account the finite width of the monochromator slit function.

In the case of overlapping, but noninteracting resonances the cross section is given[92–94] by

$$\sigma_i(E)=C+\sum_j (a_j\varepsilon_j+b_j)/(1+\varepsilon_j^2)\ , \tag{5}$$

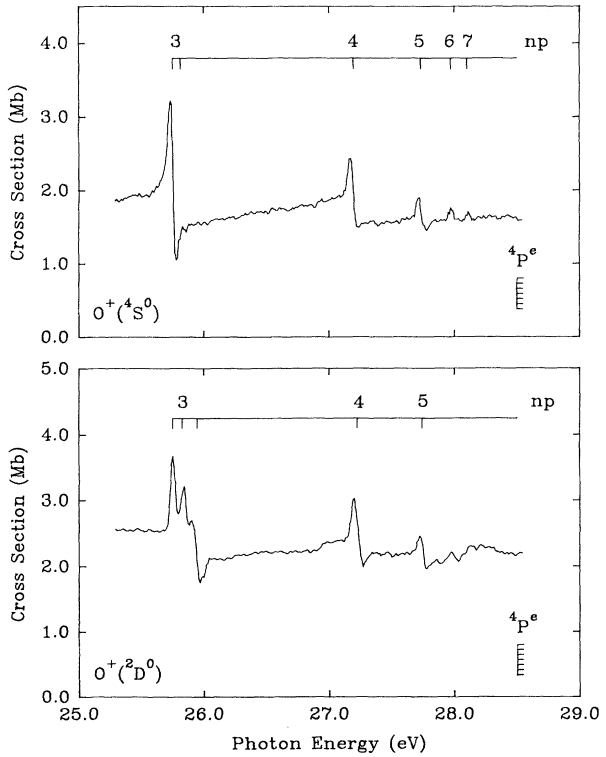

FIG. 11. Absolute photoionization cross section for the $^4S^o$ (upper panel) and $^2D^o$ (lower panel) ionic states across the $2s \rightarrow np$ ($n \geq 3$) autoionizing Rydberg series. The CIS spectra have been taken in steps of 10 meV and with a resolution of 0.7 Å. Portions of these spectra are shown in Ref. 57 at a resolution of 0.3 Å.

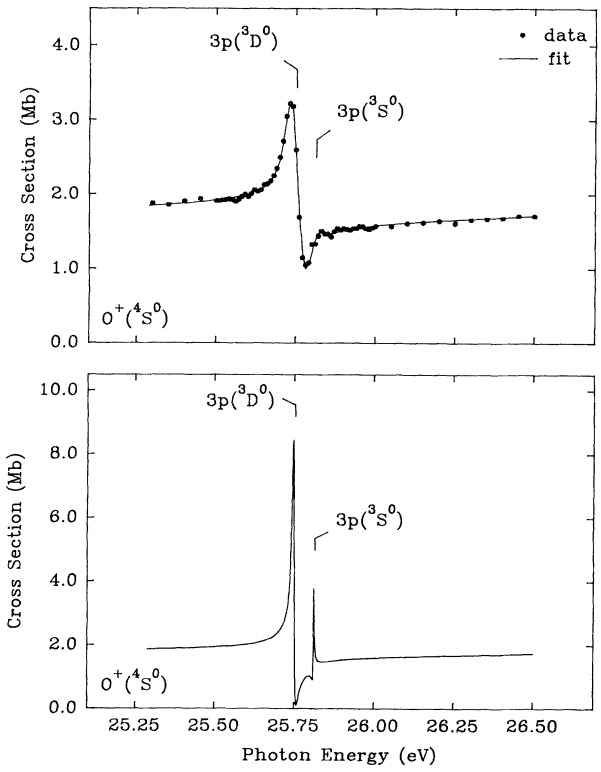

FIG. 12. Absolute photoionization cross section for the $^4S^o$ ionic state across the $2s \rightarrow 3p$ ($^3S^o,^3D^o$) autoionizing resonances. The lower panel contains the profile as calculated with the parameters in Table VI. The upper panel shows the same profile convoluted with a Gaussian of 0.71-Å FWHM, which represents the monochromator slit function, together with our experimental data points. Details of the fit procedure are described in the text.

TABLE VII. Theoretical resonance parameters for the $2s \rightarrow 3p$ ($^3S^o, ^3P^o, ^3D^o$) autoionizing Rydberg states as calculated by Taylor and Burke (Ref. 20) for the total cross section. L stands for length gauge, V for velocity gauge.

Resonance state	Energy (eV)	FWHM (meV)	q
$2s2p^4(^4P^e)3p(^3D^o)$	25.87	0.713	−1.19 (L)
			−0.54 (V)
$2s2p^4(^4P^e)3p(^3S^o)$	25.96	0.334	−2.17 (L)
			−1.53 (V)
$2s2p^4(^4P^e)3p(^3P^o)$	26.07	3.57	−0.67 (L)
			−1.25 (V)

$$\varepsilon_j = 2(E - E_j^o)/\Gamma_j \ . \tag{6}$$

In Eq. (5), $\sigma_i(E)$ is the photon-energy-dependent *partial* cross section, C stands for the nonresonant part of the cross section that varies only slowly with the photon energy E, and a_j and b_j are parameters that determine the shape of the profile. The reduced energy ε_j is the distance from the exact position E_j^o of resonance j expressed in units of its width Γ_j (FWHM).

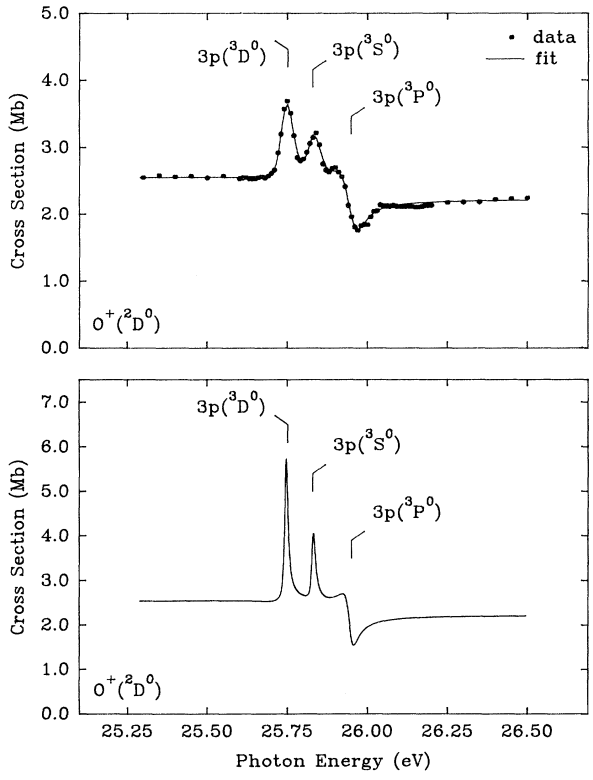

FIG. 13. Absolute photoionization cross section for the $^2D^o$ ionic state across the $2s \rightarrow 3p$ ($^3S^0, ^3P^o, ^3D^o$) autoionizing resonances. The lower panel contains the profile as calculated with the parameters in Table V. The upper panel shows the same profile convoluted with a Gaussian of 0.71 Å FWHM, which represents the monochromator slit function, together with our experimental data points. Details of the fit procedure are described in the text.

Alternatively, the cross section may be expressed as a Fano profile:[86–91]

$$\sigma_i(E) = \sigma^b + \sum_j [\sigma_j^q (q_j + \varepsilon_j)^2]/(1 + \varepsilon_j^2) \ . \tag{7}$$

In Eq. (7), σ^b is the slowly varying, nonresonant part of the cross section, σ_j^q arises from the interaction of the autoionizing Rydberg state j with the continuum, and q_j is the Fano line profile index. The q_j is related to a_j and b_j according to

$$q_j = [b_j + (a_j^2 + b_j^2)^{1/2}]/a_j \ . \tag{8}$$

The fit procedure employed a Simplex[95] algorithm in which the parameters are given a trial value first. Next, the resonance profile is calculated according to Eq. (5) and the result is convoluted with the monochromator slit function to account for the broadening of the lines. Then the root-mean-square deviation between the calculated and experimental line shapes is computed and new trial values for the parameters are obtained. The procedure is repeated iteratively until the least squares deviation is minimal.

The profiles in the $^4S^o$ and $^2D^o$ channels were fit with two and three resonances, respectively, i.e., spin-orbit coupling was neglected. The monochromator slit function was described by a Gaussian of 0.71-Å FWHM as determined by fitting the Xe $5p^6(^1S_o) \rightarrow$ Xe $5p^5(^2P_{1/2})8s'$ resonance[66] at 12.58 eV and the Ar $3s^23p^6(^1S_o) \rightarrow$ Ar $3s3p^6(^2S_{1/2})5p$ resonance[65] at 28.00 eV. Moreover, the Gaussian character and the FWHM deduced from these lines gave the lowest root-mean-square deviation in the fitting of the oxygen resonances. The results of the fit are presented in Figs. 12 and 13, and Table VI. The procedure followed is supported by the high quality of the fits.

The few calculations for the $np(^3S^o, ^3P^o, ^3D^o)$ resonances that exist[20–22,31] are mostly concerned with the total cross section. Thus a detailed comparison between experimental (Table VI) and theoretical parameters (Table VII) is not possible to date. It seems, however, that the calculated width of the resonances are about an order of magnitude too low. On the other hand, the shape of both resonances in the $^4S^o$ channel appears to be reproduced very well by the calculations by Pradhan[22] (Fig. 2). In addition, the $^3P^o$ is calculated to have the largest width,[20] which is indeed borne out by our experiment.

IV. CONCLUSIONS

By combining synchrotron radiation and photoelectron spectroscopy we performed an angle-resolved photoemission experiment on atomic oxygen over a wide energy range. Both the partial cross sections and the asymmetry parameters for the $^4S^o$ and $^2D^o$ ionic states were studied from their respective thresholds to just above the $2s^{-1}\,^4P^e$ limit. Attention was focused on the numerous autoionization resonances in this region.

The asymmetry parameter values compare favorably with the few data available from previous experiments done with line sources. Although accurate relative partial cross sections have been obtained, some ambiguity remains in putting these relative measurements on an absolute scale.

In spite of the fact that a large number of theoretical papers dealing with the photoionization of atomic oxygen have appeared in the literature, the present experiments reveal an urgent need for the calculation of *partial* cross sections and asymmetry parameters across the autoionizing resonances, which dominate the spectrum from the first ionization potential to about 30 eV.

ACKNOWLEDGMENTS

This work was supported by the U.S. Department of Energy, under Contract No. DE-AC05-84OR21400 with the Martin Marietta Energy Systems, Inc. Financial support from the Netherlands Organization for Scientific Research (PvdM) and the North Atlantic Treaty Organization under Grant No. 0404/87 is gratefully acknowledged. The Synchrotron Radiation Center is operated under National Science Foundation Grant No. DMR-8821625. The authors wish to thank professors J. W. Taylor and P. N. Schatz for the use of their beamline.

*On leave from the University of Amsterdam, Amsterdam, The Netherlands.

[1]D. R. Bates, R. A. Buckingham, H. S. W. Massey, and J. J. Unwin, Proc. R. Soc. London **170**, 322 (1939).

[2]D. R. Bates, Mon. Not. R. Astron. Soc. **100**, 25 (1939).

[3]D. R. Bates, Mon. Not. R. Astron. Soc. **106**, 423 (1946).

[4]D. R. Bates, Mon. Not. R. Astron. Soc. **106**, 432 (1946).

[5]D. R. Bates and M. J. Seaton, Mon. Not. R. Astron. Soc. **109**, 698 (1949).

[6]A. Dalgarno and D. Parkinson, J. Atmos. Terr. Phys. **18**, 335 (1960).

[7]A. Dalgarno, R. J. W. Henry, and A. L. Stewart, Planet. Space Sci. **12**, 235 (1964).

[8]R. J. W. Henry, J. Chem. Phys. **44**, 4357 (1966).

[9]R. J. W. Henry, Planet. Space Sci. **15**, 1747 (1967).

[10]R. J. W. Henry, J. Chem. Phys. **48**, 3635 (1968).

[11]E. J. McGuire, Phys. Rev. **175**, 20 (1968).

[12]R. J. W. Henry, Planet. Space Sci. **16**, 1503 (1968).

[13]G. M. Thomas and T. M. Helliwell, J. Quant. Spectrosc. Radiat. Transfer **10**, 423 (1970).

[14]J. U. Koppel, J. Chem. Phys. **55**, 123 (1971).

[15]H. Kähler, J. Quant. Spectrosc. Radiat. Transfer **11**, 1521 (1971).

[16]P. S. Ganas, Phys. Rev. A **7**, 928 (1973).

[17]A. F. Starace, S. T. Manson, and D. J. Kennedy, Phys. Rev. A **9**, 2453 (1974).

[18]S. T. Manson, D. J. Kennedy, and A. F. Starace, Planet. Space Sci. **22**, 1535 (1974).

[19]E. R. Smith, Phys. Rev. A **13**, 1058 (1976).

[20]K. T. Taylor and P. G. Burke, J. Phys. B **9**, L353 (1976).

[21]A. K. Pradhan and H. E. Saraph, J. Phys. B **10**, 3365 (1976).

[22]A. K. Pradhan, J. Phys. B **11**, L729 (1978).

[23]K. Kirby, E. R. Constantinides, S. Babeu, M. Oppenheimer, and G. A. Victor, At. Data Nucl. Data Tables **23**, 63 (1979).

[24]D. Hofsaess, At. Data Nucl. Data Tables **24**, 285 (1979).

[25]S. T. Manson, A. Msezane, A. F. Starace, and S. Shahabi, Phys. Rev. A **20**, 1005 (1979).

[26]A. K. Pradhan, Planet. Space Sci. **28**, 165 (1980).

[27]B. L. Henke, P. Lee, T. J. Tanaka, R. L. Shimabukuro, and B. K. Fujikawa, At. Data Nucl. Data Tables **27**, 1 (1982).

[28]J. J. Yeh and I. Lindau, At. Data Nucl. Tables **32**, 1 (1985).

[29]G. A. Vesnicheva, G. M. Malyshev, V. F. Orlov, and N. A. Cherepkov, Zh. Tekh. Fiz. **56**, 665 (1986) [Sov. Phys.—Tech. Phys. **31**, 402 (1986)].

[30]V. F. Orlov, N. A. Cherepkov, and L. V. Chernysheva, Opt. Spektrosck. **64**, 683 (1988) [Opt. Spectrosc. (USSR) **64**, 409 (1988)].

[31]K. L. Bell, P. G. Burke, A. Hibbert, and A. E. Kingston, J. Phys. B **22**, 3197 (1989).

[32]R. B. Cairns and J. A. R. Samson, Phys. Rev. **139**, A1403 (1965).

[33]R. E. Huffman, J. C. Larrabee, and Y. Tanaka, J. Chem. Phys. **46**, 2213 (1967).

[34]R. E. Huffman, J. C. Larrabee, and Y. Tanaka, J. Chem. Phys. **47**, 4462 (1967).

[35]M. E. Rudd and K. Smith, Phys. Rev. **169**, 79 (1968).

[36]F. J. Comes, F. Speier, and A. Elzer, Z. Naturforsch. A **23**, 125 (1968).

[37]N. Jonathan, D. J. Smith, and K. J. Ross, J. Chem. Phys. **53**, 3758 (1970).

[38]N. Jonathan, A. Morris, D. J. Smith, and K. J. Ross, Chem. Phys. Lett. **7**, 497 (1970).

[39]R. A. van Tassel, R. E. Huffman, and J. L. Roebber, J. Chem. Phys. **59**, 5926 (1971).

[40]P. M. Dehmer, J. Berkowitz, and W. A. Chupka, J. Chem. Phys. **59**, 5777 (1973).

[41]J. A. R. Samson and V. E. Petrosky, Phys. Rev. A **9**, 2449 (1974).

[42]J. A. R. Samson and V. E. Petrosky, J. Electron Spectrosc. Relat. Phenom. **3**, 461 (1974).

[43]P. M. Dehmer and W. A. Chupka, J. Chem. Phys. **62**, 584 (1975).

[44]W. H. Hancock and J. A. R. Samson, J. Electron Spectrosc. Relat. Phenom. **9**, 211 (1976).

[45]C. E. Moore, *Selected Tables of Atomic Spectra,* Natl. Bur. Stand. Ref. Data Ser., Natl. Bur. Stand. (U.S.) Circ. No. 3 (U.S. GPO, Washington, D.C., 1976), Sec. 7.

[46]P. M. Dehmer, W. L. Luken, and W. A. Chupka, J. Chem. Phys. **67**, 195 (1977).

[47]J. A. R. Samson and W. H. Hancock, Phys. Lett. **61A**, 380 (1977).

[48]J. L. Dehmer and P. M. Dehmer, J. Chem. Phys. **67**, 1782 (1977).

[49]J. L. Kohl, G. P. Lafyatis, H. P. Palenius, and W. H. Parkinson, Phys. Rev. A **18**, 571 (1970).

[50]D. M. de Leeuw and C. A. de Lange, Chem. Phys. **54**, 123

(1980).
[51]R. L. Kelly, Oak Ridge National Laboratory Report No. 5922, 1982.
[52]M. I. A. Hussein, D. M. P. Holland, K. Codling, P. R. Woodruff, and E. Ishiguro, J. Phys. B **18**, 2827 (1985).
[53]J. A. R. Samson and P. N. Pareek, Phys. Rev. A **31**, 1470 (1985).
[54]J. A. R. Samson and G. C. Angel, X-Ray and Vacuum Ultraviolet Interaction Data Bases, Calculations and Measurements [Proc. SPIE **911**, 80 (1988)].
[55]W. J. van der Meer, P. van der Meulen, M. Volmer, and C. A. de Lange, Chem. Phys. **126**, 385 (1988).
[56]G. C. Angel and J. A. R. Samson, Phys. Rev. A **38**, 5578 (1988).
[57]P. van der Meulen, C. A. de Lange, M. O. Krause, and D. C. Mancini, Phys. Scr. **41**, 837 (1990).
[58]M. J. Seaton, in *Recent Studies in Atomic and Molecular Processes,* edited by A. E. Kingston (Plenum, New York, 1987), p. 29.
[59]M. C. Cockett, Ph.D. thesis, University of Southampton, Southampton, United Kingdom, 1990.
[60]M. O. Krause, T. A. Carlson, and P. R. Woodruff, Phys. Rev. A **24**, 1374 (1981).
[61]M. O. Krause, T. A. Carlson, and A. Fahlman, Phys. Rev. A **30**, 1316 (1984).
[62]M. O. Krause, in *Synchrotron Radiation Research,* edited by H. Winick and S. Doniach (Plenum, New York, 1980), p. 101.
[63]H. van Lonkhuyzen, Ph.D. thesis, Free University, Amsterday, The Netherlands, 1984.
[64]M. O. Krause, F. Cerrina, and A. Fahlman, Phys. Rev. Lett. **50**, 1118 (1983).
[65]R. P. Madden, D. L. Ederer, and K. Codling, Phys. Rev. **177**, 136 (1969).
[66]J. Wu, S. B. Whitfield, C. D. Caldwell, M. O. Krause, P. van der Meulen, and A. Fahlman, Phys. Rev. A **42**, 1350 (1990).
[67]J. Kreile and A. Schweig, J. Electron Spectrosc. Relat. Phenom. **20**, 191 (1980).
[68]D. M. P. Holland, A. C. Parr, D. L. Ederer, J. L. Dehmer, and J. B. West, Nucl. Instrum. Methods **195**, 331 (1982).
[69]M. O. Krause, Phys. Fennica **9**, Suppl. S1, 281 (1974).
[70]J. B. West and J. Morton, At. Data Nucl. Data Tables **22**, 103 (1978).
[71]G. V. Marr and J. B. West, At. Data Nucl. Data Tables **18**, 497 (1976).
[72]J. E. Collin and P. Natalis, Int. J. Mass Spectrom. Ion Phys. **2**, 231 (1969).
[73]A. L. Smith, Philos. Trans. R. Soc. London. Ser. A **268**, 169 (1970).
[74]A. L. Smith, J. Quant. Spectrosc. Radiat. Transfer **10**, 1129 (1970).
[75]J. L. Bahr, A. J. Blake, J. H. Carver, J. L. Gardner, and V. Kumar, J. Quant. Spectrosc. Radiat. Transfer **11**, 1853 (1971).
[76]J. A. Kissinger and J. W. Taylor, Int. J. Mass Spectrom. Ion Phys. **11**, 461 (1973).
[77]K. Tanaka and I. Tanaka, J. Chem. Phys. **59**, 5042 (1973).
[78]P. M. Dehmer and W. A. Chupka, J. Chem. Phys. **62**, 4525 (1975).
[79]J. A. R. Samson and J. L. Gardner, J. Chem. Phys. **67**, 755 (1977).
[80]J. L. Gardner and J. A. R. Samson, J. Electron Spectrosc. Relat. Phenom. **13**, 7 (1978).
[81]J. H. D. Eland, J. Chem. Phys. **72**, 6015 (1980).
[82]A. Tabché-Fouhaile, I. Nenner, P.-M. Guyon, and J. Delwiche, J. Chem. Phys. **75**, 1129 (1981).
[83]P. Morin, I. Nenner, M. Y. Adam, M. J. Hubin-Franskin, J. Delwiche, H. Lefebvre-Brion, and A. Giusti-Suzor, Chem. Phys. Lett. **92**, 609 (1982).
[84]D. M. P. Holland and J. B. West, Z. Phys. D **4**, 367 (1987).
[85]C. Y. R. Wu, J. Quant. Spectrosc. Radiat. Transfer **37**, 1 (1987).
[86]U. Fano, Phys. Rev. **124**, 1866 (1961).
[87]U. Fano and J. W. Cooper, Phys. Rev. **137**, A1364 (1965).
[88]U. Fano and J. W. Cooper, Rev. Mod. Phys. **40**, 441 (1968).
[89]M. J. Seaton, Rep. Prog. Phys. **46**, 167 (1983).
[90]K. Ueda, Phys. Rev. A **35**, 2484 (1987).
[91]K. Ueda, K. Maeda, K. Ito, and T. Namioka, J. Phys. B **22**, L481 (1989).
[92]B. W. Shore, Rev. Mod. Phys. **39**, 439 (1967).
[93]B. W. Shore, J. Opt. Soc. Am. **57**, 881 (1967).
[94]B. W. Shore, Phys. Rev. **171**, 43 (1968).
[95]J. A. Nelder and R. Mead, Comput. J. **7**, 308 (1964).